





Critical magnetic behavior in $[\text{Ag}_8/\text{Co}_{0.5}]_{\text{x}64}$, $[\text{Ag}_8/\text{Co}_1]_{\text{x}32}$ and $[\text{Ag}_{16}/\text{Co}_1]_{\text{x}32}$ epitaxial multilayers

Cite as: AIP Advances **11**, 025220 (2021); <https://doi.org/10.1063/9.0000086>

Submitted: 16 October 2020 . Accepted: 22 January 2021 . Published Online: 08 February 2021

Enrique Navarro, María Alonso, Ana Ruiz, Cesar Magen, Unai Urdiruz,  Federico Cebollada, Lluís Balcells,  Benjamín Martínez,  Jesús M. González, and  F. Javier Palomares

COLLECTIONS

Paper published as part of the special topic on [65th Annual Conference on Magnetism and Magnetic Materials](#), [65th Annual Conference on Magnetism and Magnetic Materials](#), [65th Annual Conference on Magnetism and Magnetic Materials](#), [65th Annual Conference on Magnetism and Magnetic Materials](#), [65th Annual Conference on Magnetism and Magnetic Materials](#) and [65th Annual Conference on Magnetism and Magnetic Materials](#)



View Online



Export Citation



CrossMark

ARTICLES YOU MAY BE INTERESTED IN

[Temperature dependence of the magnetic interactions taking place in monodisperse magnetite nanoparticles having different morphologies](#)

AIP Advances **11**, 015025 (2021); <https://doi.org/10.1063/9.0000089>

[Low temperature superspin glass behavior in a Co/Ag multilayer](#)

AIP Advances **9**, 125327 (2019); <https://doi.org/10.1063/1.5130158>

[Solid-state cooling by stress: A perspective](#)

Applied Physics Letters **116**, 050501 (2020); <https://doi.org/10.1063/1.5140555>



Critical magnetic behavior in $[Ag_8/Co_{0.5}]_x64$, $[Ag_8/Co_1]_x32$ and $[Ag_{16}/Co_1]_x32$ epitaxial multilayers

Cite as: AIP Advances 11, 025220 (2021); doi: 10.1063/9.0000086

Presented: 2 November 2020 • Submitted: 16 October 2020 •

Accepted: 22 January 2021 • Published Online: 8 February 2021



Enrique Navarro,¹ María Alonso,¹ Ana Ruiz,¹ Cesar Magen,² Unai Urdiroz,¹ Federico Cebollada,³  Lluís Balcells,⁴ Benjamín Martínez,⁴  Jesús M. González,^{1,a)}  and F. Javier Palomares¹ 

AFFILIATIONS

¹Nanostructures and Surfaces, Instituto de Ciencia de Materiales de Madrid, 28049 Madrid, Spain

²Departamento de Materiales Magnéticos, Instituto de Ciencia de Materiales de Aragón, 50009 Zaragoza, Spain

³POEMMA-CEMDATIC, Universidad Politécnica de Madrid, 28040 Madrid, Spain

⁴Magnetic Materials and Functional Oxides, Institut de Ciència de Materials de Barcelona, 08193 Barcelona, Spain

Note: This paper was presented at the 65th Annual Conference on Magnetism and Magnetic Materials.

^{a)}Author to whom correspondence should be addressed: jm.g@csic.es

ABSTRACT

We investigate the low temperature magnetic behavior of three epitaxial Co/Ag multilayers, grown onto MgO (001) substrates, with a nominal content per period of either half a monolayer or one monolayer of Co, and either 8 or 16 Ag monolayers. The samples were studied by X-ray reflectivity and diffraction, transmission electron microscopy, magnetometry and ac susceptometry. The results indicated a well defined stacking sequence in the growth direction, the number of periods and of Ag monolayers per period being coincident with the nominal values for each sample. The Co layers were found to be discontinuous and corresponded to a quasi-monodisperse in-plane distribution of Co nanoparticles embedded in a Ag(001) matrix. The zero-field cooled and field cooled temperature variations of the low field magnetization indicated the presence of irreversibilities at temperatures below 20 K. The ac field frequency (f) and temperature (T) dependencies of the real part of the susceptibility (χ') corresponded to a Vogel-Fulcher behavior in the three samples, and indicated a frequency shift parameter (T) of the order of 4×10^{-2} . For each sample, the experimental data corresponding to the variations of the imaginary part of the ac susceptibility (χ'') with f and T were found to collapse into a single curve according to the dynamic scaling law. Taken together, these results allow us to conclude that the three multilayers experience a phase transition of the paramagnetic to superspin glass type, driven by the dipolar interactions between the Co nanoparticles. Regarding the influence of the multilayer features, we found a clear dependence of the order parameter of the transition on the nominal number of Co monolayers per period.

© 2021 Author(s). All article content, except where otherwise noted, is licensed under a Creative Commons Attribution (CC BY) license (<http://creativecommons.org/licenses/by/4.0/>). <https://doi.org/10.1063/9.0000086>

INTRODUCTION

Quenched disorder and competing interactions coexisting in a system constitute the necessary ingredients for the occurrence of the so-called spin glass behavior.¹ That behavior is largely ubiquitous and has been identified in many different fields,¹ like the analysis of the human brain functionality,² neural networks,^{3,4} prebiotic evolution⁵ or protein folding.⁶ Nevertheless, the paradigm of the spin glass phenomenology and of its theoretical understanding

are magnetic moments systems including distributed interactions. Actual realizations of magnetic spin glass systems include from the simple canonical spin glass metallic phases (where diluted, randomly distributed, localized moments interact through the spatially oscillatory RKKY interaction), to more complex magnetic materials incorporating different inter-moments interactions (from super- and double-exchange to dipolar coupling). The magnetic spin glass systems also encompass a broad range of dimensionalities, disorder types and disorder parameters distributions.^{1,7,8} In a previous work⁹

on a Co/Ag multilayer with granular morphology at the Co layers, we have shown the occurrence at low temperature of a superspin glass phase transition governed by the dipolar interactions between the freezing Co nanoparticles. Here we extend the analysis of the low temperature magnetic behavior to a series of Co/Ag multilayers also including a reduced Co content per period and explore the influence of varying the Co or Ag content per period.

SAMPLE PREPARATION AND EXPERIMENTAL TECHNIQUES

The three multilayers ($[\text{Ag}_8/\text{Co}_{0.5}] \times 64$, $[\text{Ag}_8/\text{Co}_1] \times 32$ and $[\text{Ag}_{16}/\text{Co}_1] \times 32$) have been grown by molecular beam epitaxy (MBE), alternating Ag and Co deposition on clean MgO(001) surfaces.

Samples were covered by a 3 nm Ag capping layer, and, in the following, will be termed X/Y, X being the nominal number of Co monolayers (ML) per period, and Y that of Ag ones. Here X is either 0.5 or 1 Co ML, while Y is either 8 or 16 Ag ML. In order to deposit the same total nominal number of Co atoms per surface unit at the three samples, the period was repeated 32 or 64 times depending on the X value (1 or 0.5). The stacking, structure and morphology of the samples were investigated by means of X-rays reflectivity (XRR), diffraction (XRD) and scanning transmission electron microscopy (STEM). The magnetic characterization was performed by using vibrating sample and SQUID magnetometers (fields of up to 90 kG) and an ac susceptometer, covering the range of ac field frequencies (f) from 10^{-1} up to 10^4 Hz, and temperatures (T) from 2 K up to 290 K.

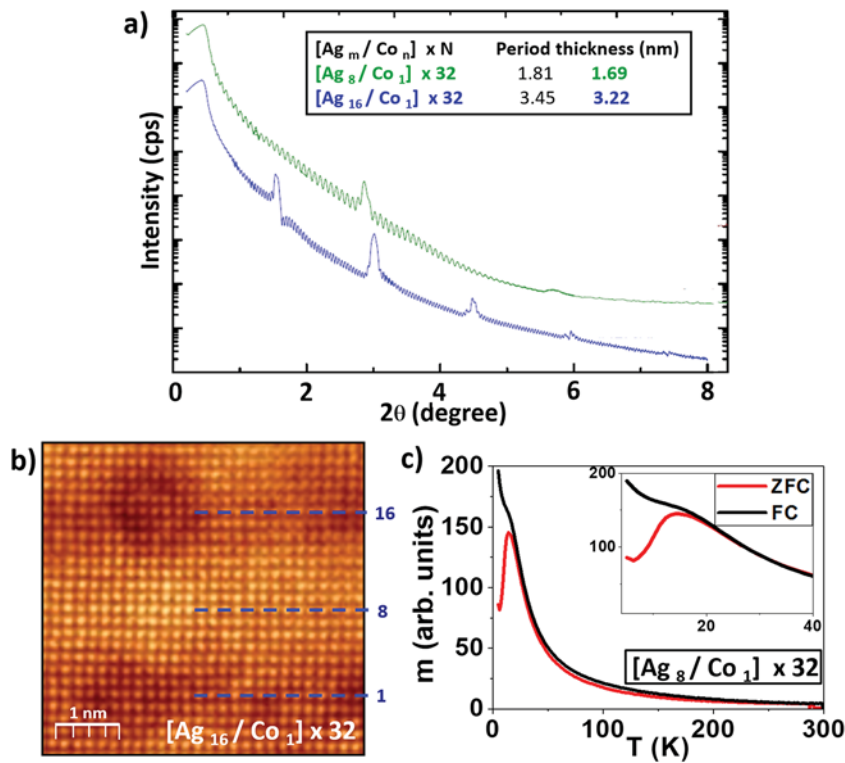


FIG. 1. a) XRR results for the 1/8 and 1/16 samples, indicating also the nominal values of the period thickness (black figures) and those derived from the XRR analysis (green/blue figures); b) High resolution cross section STEM image of the 1/16 sample showing Co NPs (dark) embedded in a Ag (001) matrix; data correspond to two consecutive Co layers separated by 16 Ag monolayers (numbers in blue); c) ZFC/FC curves of the dc low field magnetization vs T for the 1/8 sample.

TABLE I. Values of different parameters derived from the magnetic analysis for each sample (details in the text). T_{irr} : irreversibility temperature observed at the ZFC/FC low field magnetization curves; V_{para} and ϕ_{para} : paramagnetic average volume and diameter estimated for the Co nanoparticles from the Curie–Weiss fits; Γ : frequency shift parameter; T_0 and E_a/k_B : magnitude of the interactions and activation energy for system relaxation, respectively (Vogel–Fulcher model); $Z\nu$ (critical exponent) and T_g (phase transition temperature for an infinite observation time) obtained from the fit of the ac susceptibility to the scaling law at the critical regime.

Co/Ag sample	T_{irr} (K)	$V_{\text{para}} \times 10^{-21}$ (cm ³)	ϕ_{para} (nm)	$\Gamma \times 10^{-2}$	T_0 (K)	E_a/k_B (K)	$Z\nu$	T_g (K)
0.5/8	11.0	1.2	1.3 ± 0.2	4.0	7.1	37.6	9.0	8.1
1/8	17.8	3.4	1.9 ± 0.2	4.9	10.3	45.7	9.6	15.5
1/16	14.0	3.3	1.9 ± 0.2	4.7	14.3	62.1	6.7	12.0

RESULTS AND DISCUSSION

The XRD, XRR, and STEM results indicated that the MBE deposited films exhibited good crystallinity, fcc(001) structure and clear superlattice periodicities, the number of periods in each sample being coincident with the nominal ones (see e.g., the XRR data shown in Figure 1a for the 1/8 and 1/16 samples). The STEM images also revealed that, as reported in Ref. 9, the Co layers were not continuous (see Fig. 1b), but exhibited a close-to-monodisperse in-plane distribution of Co nanoparticles (NPs) embedded in a Ag(001) matrix. The characteristic size and shape of the Co NPs for the 1/16 sample can be seen in Figure 1b, which also shows the presence of 16 Ag MLs between two consecutive Co layers. The STEM analysis of the different samples indicated a disordered distribution of the Co NPs positions within each layer, and confirmed the nominal Ag periodicity. For the 1/8 and 1/16 samples, the distance between the

lateral surfaces of two neighboring NPs in a Co layer is of the order of 1.5 nm, similar to the average NPs diameter.

The zero field-cooling (ZFC) and field-cooling (FC) variations with T of the dc low field magnetization indicated the occurrence of irreversibilities at temperatures (T_{irr}) lower than 20 K (see Fig. 1c for the 1/8 sample, and T_{irr} values for each sample in Table I). Below T_{irr} , the multilayers exhibited hysteresis with dc coercivities of up to 350 Oe at 2 K. Above T_{irr} , the ZFC initial dc susceptibility (χ) behaved according to the Curie–Weiss law,¹⁰ $1/\chi = (T - \theta)/C$, in the three samples. The values obtained from the fits to the Curie–Weiss law yielded paramagnetic moments two orders of magnitude larger than the Co atomic moment. They approximately correspond to the clustering of fcc coordinated Co moments in a NP with a diameter between 1 and 2 nm. Since this is consistent with the granular morphology of the Co layers revealed by STEM, these Curie–Weiss paramagnetic moments can be associated to the Co NPs and we used

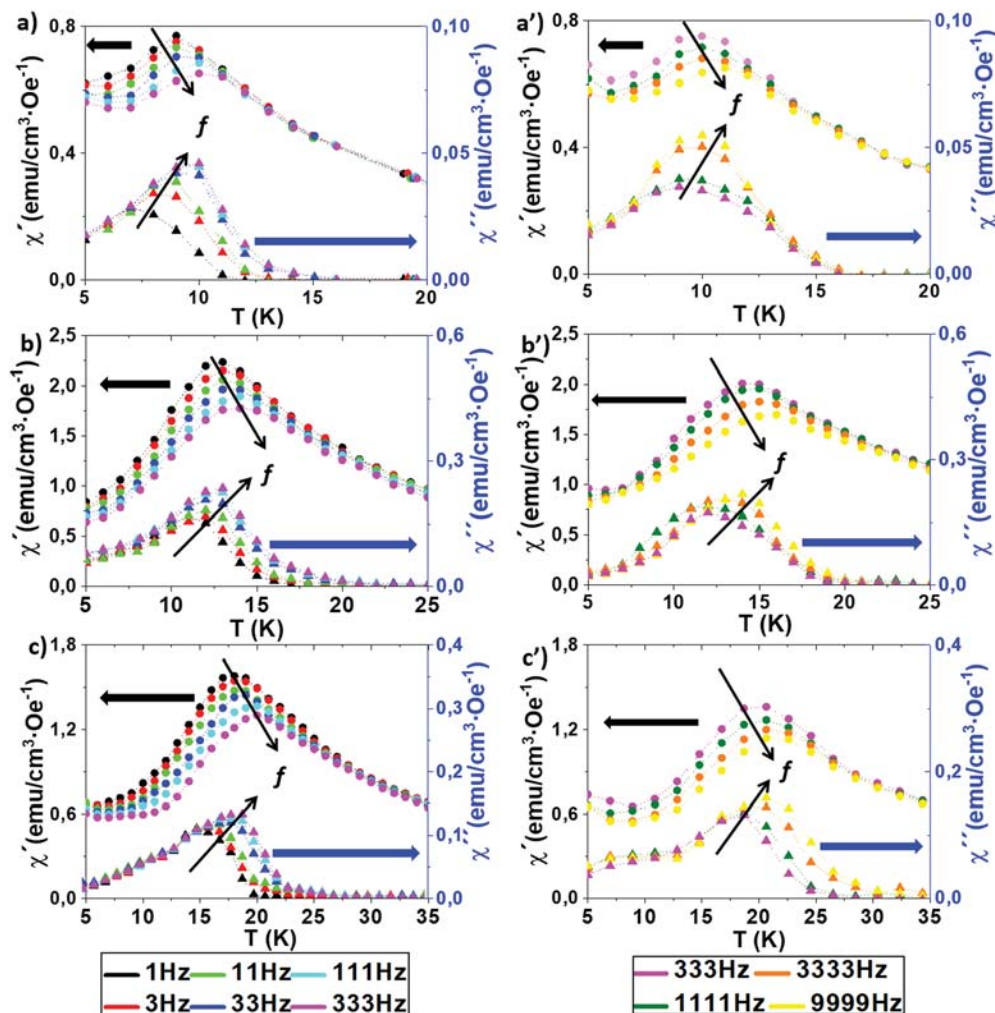


FIG. 2. Temperature dependencies of the real (χ') and imaginary (χ'') components of the ac susceptibility measured at the indicated frequencies, by using a SQUID magnetometer (left panels) or an ac susceptometer (right panels); a)-a') display data for 0.5/8 sample, b)-b') for 1/16 sample, and c)-c') for 1/8 sample.

them to estimate the average volumes (V_{para}) and diameters (ϕ_{para}) of the NPs (assumed spherical); see values in Table I.

Figure 2 shows the temperature dependencies of the real (χ') and imaginary (χ'') parts of the ac susceptibility¹ measured at ac field frequencies (f) in the range from 1 Hz up to 10 kHz. Maxima on χ' are observed at temperatures ($T_{p,ac}$) of the order of T_{irr} . $T_{p,ac}$ and their associated peak magnitudes increase and decrease, respectively, as f increases. The variations of $T_{p,ac}$, with f are parameterized¹ by considering the relative increase of $T_{p,ac}$ per decade, according to $\Gamma = (\Delta T_{p,ac}/T_{p,ac})/\Delta \log_{10} f$, and taking as reference $f = 1$ Hz. The Γ values thus obtained (see Table I) are clearly lower than those associated to superparamagnetic relaxation processes (which in a large majority of materials are above 0.2¹). These results suggest that, like in our previous report,⁹ the magnetic properties of these multilayers are associated to the Co NPs of the nominal Co layers, and that such NPs could exhibit at T_{irr} a phase transition from a paramagnetic to a magnetically ordered state.

In order to assess the actual occurrence of interactions between the Co NPs, we have fitted the experimental data for the frequency variation of $T_{p,ac}$ to the Vogel–Fulcher model.¹¹ That model describes the temperature dependence of the characteristic times of the spin glass-like freezing¹² according to $\omega = \omega_0 \exp[-E_a/k_B(T_{p,ac} - T_0)]$, where ω is the ac field angular frequency and ω_0 , E_a , and T_0 fitting parameters: ω_0 is the try frequency, E_a the activation energy for the relaxation, and T_0 the magnitude (in temperature units) of the interactions present in the system; Table I

shows the T_0 and E_a/k_B values obtained from the fits. For the three samples, ω_0 values are in the range of $5 \times 10^9 \text{ s}^{-1}$, whereas T_0 values are of the order of the corresponding T_{irr} . Thus, these results clearly endorse the presence of interactions whose magnitude could be on the origin of an ordered magnetic state at temperatures below T_{irr} , transitioning to a superparamagnetic phase above T_{irr} .

To analyze that behavior we will consider two different approaches. First, we will study the relationship of the temperature relaxation time $\tau(T)$ with the $T_{p,ac}$ experimentally determined values.^{1,13,14} That relationship can only be established at the critical state, that is, at T near the phase transition at which the distribution of the magnetically correlated regions (through the interactions present in the system) spans all the possible dimensions compatible with the elemental interacting entities and the system sizes. The lifetimes of the correlated regions should also reach the characteristic time of the measurement. In this critical state, the spin relaxation time diverges with the reduced correlation length (ξ) according to $\tau = \tau_0^* \xi^Z$ (where Z is the dynamic scaling exponent). ξ is related to $T_{p,ac}$ through the law $\xi = \varepsilon^{-\nu}$ (where ν measures the divergence of the correlation length, and $\varepsilon = [(T_{p,ac}/T_g)-1]$; T_g being the temperature at which the phase transition occurs when the measuring time is infinite. In terms of the frequency f , the scaling law takes the form: $f = f^* [(T_{p,ac}/T_g)-1]^{Z\nu}$ or equivalently, $\ln f = \ln f^* - Z\nu \ln [(T_{p,ac}/T_g)-1]$ ($Z\nu$ is the exponent linked to the collective state occurring below T_g). Figure 3a) displays, for the three multilayers, the dependence of the logarithm of the frequency f on the

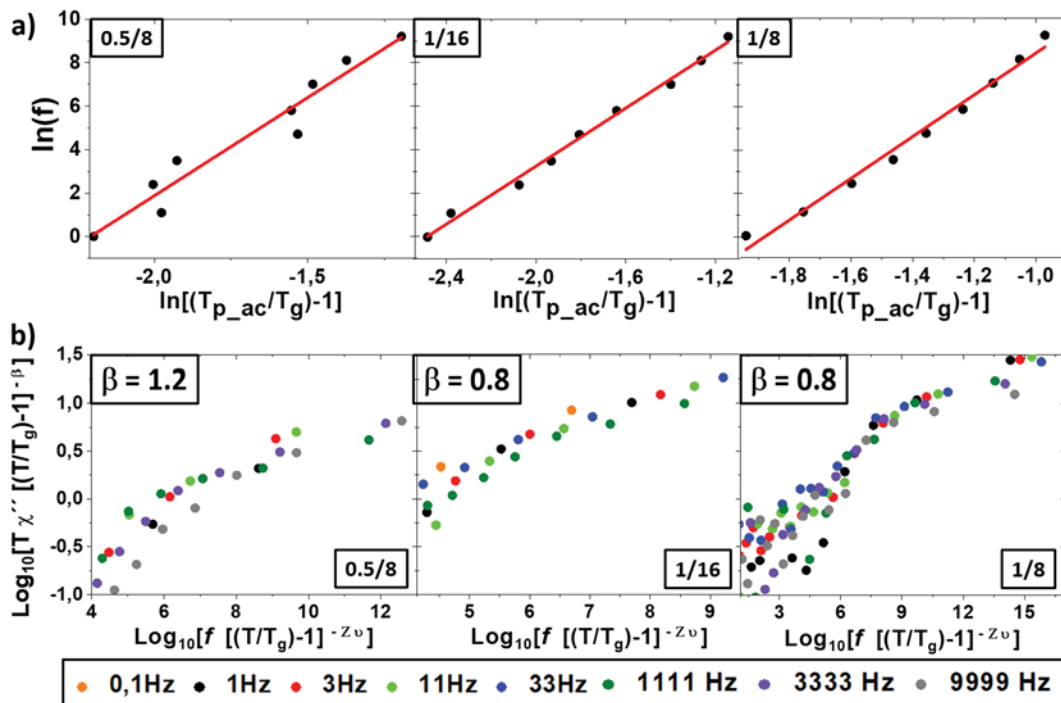


FIG. 3. a) Dependence of the logarithm of the ac field frequency (f) on the quantity $\ln[(T_{p,ac}/T_g)-1]$ for each sample; b) Collapse of the experimental data from the f and T dependencies of the absorption component of the ac susceptibility (χ'') according to the dynamic scaling law (see text).

quantity $\ln[(T_{p,ac}/T_g)-1]$; the f^* values considered for the three samples were of the order of 10^9 s^{-1} ; those of the $Z\nu$ and T_g parameters are shown in Table I. As it is readily seen, in all the cases there is a good agreement between the experimental data and the scaling law. It is interesting to remark that the T_g values are slightly lower than the T_{irr} ones (as expected from the finite measuring times). Also, and importantly, the values of the critical exponent here obtained (varying from $Z\nu = 6.7$ to 9.6 ; see Table I) are clearly within the range identified in the literature as corresponding to the occurrence of spin glass-like systems freezing.^{15–17}

Our second approach to elucidate if a freezing transition occurs in these samples at T_{irr} , is based on the dynamic scaling of the imaginary (absorption) component of the ac susceptibility (χ'').¹⁸ That scaling predicts the collapse of the experimental data corresponding to the f and T variations of χ'' , in a single curve $G(x)$, verifying: $T \chi''(f, T) = [(T/T_g) - 1]^\beta G(x)$; in this expression $x = f[(T/T_g) - 1]^{-Z\nu}$ (where $Z\nu$ is the critical exponent and T_g is the transition temperature at zero frequency); β is the order parameter of the transition.¹ Figure 3(b) displays the scaling behavior obtained for our three samples, which is in agreement with the existence of a freezing transition at temperatures close to T_{irr} . Note that the β values, obtained from the collapse in Figure 3, are in the range corresponding to spin glass-like systems.¹⁸ Interestingly, in these samples the β values are only found to vary with the nominal number of Co monolayers per period.

CONCLUSIONS

The above results allow us to conclude that the three multilayers experience a phase transition of the paramagnetic to super-spin glass type at temperatures T_{irr} . The freezing entities are the Co nanoparticles present at the nominal Co layers. The magnitude of the moments of these Co NPs, as well as that of the average interparticle distance, indicate the occurrence of high dipolar interactions. We thus propose that such interactions, together with the in-plane disorder of the NP positions, are on the origin of the spin glass-like magnetic order.⁹ The size and in-plane concentration of the Co NPs can be also correlated with the variations observed in T_{irr} depending on the nominal number of Co and Ag monolayers per period. It can be seen that the 0.5/8 sample exhibits a lower T_{irr} than the 1/8 and 1/16 samples; this is due to the smaller volume and in-plane concentration of the Co NPs present in the 0.5/8 sample, and the consequently lower magnitude of the interparticle dipolar interactions. On the other hand, our results indicate that the 1/8 sample experiences the phase transition at a higher temperature than the 1/16 sample; this can be explained by considering the thickness of the Ag spacer, which for the 1/16 sample is large enough to significantly reduce the interlayer Co NPs interactions; in contrast, those interlayer interactions measurably contribute to the phase transition in the 1/8 sample. Finally, the values of the β exponent in the scaling relationship are only found to vary (in these samples) with the number of Co monolayers per period.

ACKNOWLEDGMENTS

This work has been developed with funds corresponding to project MAT2016-80394-R financed by the Spanish Research Agency (AEI). We also acknowledge the Spanish Ministerio de Ciencia e Innovación and Consejo Superior de Investigaciones Científicas for financial support and for provision of synchrotron radiation at beamline BM25-SpLine (ESRF).

DATA AVAILABILITY

The data that support the findings of this study are available from the corresponding author upon reasonable request.

REFERENCES

- J. A. Mydosh, *Spin Glasses: An Experimental Introduction* (CRC Press, London; Washington, DC, 1993).
- J. J. Hopfield, "Neural networks and physical systems with emergent collective computational abilities," *PNAS* **79**, 2554–2558 (1982).
- H. Sompolinsky, "Statistical mechanics of neural networks," *Phys. Today* **41**(12), 70 (1988).
- D. W. Tank and J. J. Hopfield, "Collective computation in neuronlike circuits," *Scientific American* **257**(6), 104–115 (1987).
- S. Kauffman, *The Origins of Order: Self-Organization and Selection in Evolution* (Oxford University Press, New York, 1993).
- J. D. Bryngelson and P. G. Wolynes, "Spin glasses and the statistical mechanics of protein folding," *PNAS* **84**(21), 7524–7528 (1987).
- W. Wang, M. Wallin, and J. Lidmar, "Chaotic temperature and bond dependence of four-dimensional Gaussian spin glasses with partial thermal boundary conditions," *Phys. Rev. E* **98**, 062122 (2018).
- M. C. Alocén, P. Agudo, A. Hernando, J. M. González, and P. Crespo, "Two routes to disorder in a system with competitive interactions," *J. Magn. Magn. Mater.* **242–245**, 879–881 (2002).
- E. Navarro, M. Alonso, A. Ruiz, C. Magen, U. Urdirro, F. Cebollada, L. Balcells, B. Martínez, F. J. Palomares, and J. M. González, "Low temperature superspin glass behavior in a Co/Ag multilayer," *AIP Advances* **9**, 125327 (2019).
- E. P. Wohlfarth, *Ferromagnetic Materials* (North-Holland Publishing Company, 1980), Vol. 1.
- S. Shtrikman and E. P. Wohlfarth, "The theory of the Vogel-Fulcher law of spin glasses," *Physics Letters A* **85**(8–9), 467–470 (1981).
- P. G. Debenedetti and F. H. Stillinger, "Supercooled liquids and the glass transition," *Nature* **410**, 259–267 (2001).
- P. C. Hohenberg and B. I. Halperin, "Theory of dynamic critical phenomena," *Reviews of Modern Physics* **49**(3), 435 (1977).
- A. T. Ogielski, "Dynamics of three-dimensional Ising spin glasses in thermal equilibrium," *Physical Review B* **32**(11), 7384 (1985).
- S. Ghara, B. G. Jeon, K. Yoo, K. H. Kim, and A. Sundaresan, "Reentrant spin-glass state and magnetodielectric effect in the spiral magnet $\text{BiMnFe}_2\text{O}_6$," *Physical Review B* **90**(2), 024413 (2014).
- A. Malinowski, V. L. Bezusyy, R. Minikayev, P. Dziawa, Y. Syryanyy, and M. Sawicki, "Spin-glass behavior in Ni-doped $\text{La}_{1.85}\text{Sr}_{0.15}\text{CuO}_4$," *Physical Review B* **84**(2), 024409 (2011).
- J. Lago, S. J. Blundell, A. Eguia, M. Jansen, and T. Rojo, "Three-dimensional Heisenberg spin-glass behavior in $\text{SrFe}_{0.90}\text{Co}_{0.10}\text{O}_{3.0}$," *Physical Review B* **86**(6), 064412 (2012).
- P. Beauvillain, C. Dupas, J. P. Renard, and P. Veillet, "Experimental study of the spin freezing in an insulating spin-glass: Static and dynamical aspects," *Physical Review B* **29**(7), 4086 (1984).